Hindawi
Advances in Civil Engineering
Volume 2020, Article ID 8862827, 15 pages
https://doi.org/10.1155/2020/8862827

Research Article

A Comparative Study on the V_{S30} and N_{30} Based Seismic Site Classification in Kahramanmaras, Turkey

Dalia Munaff Naji,[1] **Muge K. Akin**,[2] **and Ali Firat Cabalar**[3]

[1]*Department of Civil Engineering, Al-Mustansiriyah University, Baghdad, Iraq*
[2]*Department of Civil Engineering, Abdullah Gul University, Kayseri, Turkey*
[3]*Department of Civil Engineering, University of Gaziantep, Gaziantep, Turkey*

Correspondence should be addressed to Ali Firat Cabalar; cabalar@gantep.edu.tr

Received 7 May 2020; Revised 18 September 2020; Accepted 19 October 2020; Published 4 November 2020

Academic Editor: Hayri Baytan Ozmen

Assessment of seismic site classification (SSC) using either the average shear wave velocity (V_{S30}) or the average SPT-N values (N_{30}) for upper 30 m in soils is the simplest method to carry out various studies including site response and soil-structure interactions. Either the V_{S30}- or the N_{30}-based SSC maps designed according to the National Earthquake Hazards Reduction Program (NEHRP) classification system are effectively used to predict possible locations for future seismic events. The main goal of this study is to generate maps using the Geographic Information System (GIS) for the SSC in Kahramanmaras city, influenced by both East Anatolian Fault and Dead Sea Fault Zones, using both V_{S30} and N_{30} values. The study also presents a series of GIS maps produced using the shear wave velocity (V_S) and SPT-N values at the depths of 5 m, 10 m, 15 m, 20 m, and 25 m. Furthermore, the study estimates the bed rock level and generates the SSC maps for the average V_S values through overburden soils by using the NEHRP system. The V_{S30} maps categorize the study area mainly under class C and limited number of areas under classes B and D, whereas the N_{30} maps classify the study area mainly under class D. Both maps indicate that the soil classes in the study area are different to a high extent. Eventually, the GIS maps complied for the purpose of urban development may be utilized effectively by engineers in the field.

1. Introduction

Seismic site classification (SSC), which defines engineering properties of the soils by means of V_S or SPT-N values, is the simplest method to consider the site effects for numerous purposes including engineering projects and microzonation studies [1]. Many classification systems utilize the SPT-N and V_S values measured in upper 30 m to provide an SSC assessment [2–4]. The National Earthquake Hazard Reduction Program (NEHRP), which is one of the widely used systems for the SSC applications, classified the soils by using their V_S values in designing building codes and characterizing site response [5, 6].

The objective of this study is to make an SSC assessment in the city of Kahramanmaras located in a seismically active region in southern-central Turkey. The region is influenced by the Eastern Anatolian Fault (EAF) and the Dead Sea Fault (DSF) [7]. No studies using SPT-N values have been performed in the city and vicinity area, although little efforts have been made using V_{S30} values obtained in the city centre [8]. Variations in the soil classification have been investigated at the depths of 5 m, 10 m, 15 m, 20 m, and 25 m by producing GIS maps for both the V_S and SPT-N values obtained in the study area. The subsoil exploration has been conducted by means of seismic surface wave techniques (Multichannel Analysis of Surface Waves, MASW, and Microtremor Array Measurements, MAM) at 287 boreholes in 98 sites. The GIS maps of both weathered and engineering bed rock levels and average V_S in overburden soils have also been produced for further studies. The present study is thought to be the first investigation carried out to estimate the SSC using both V_{S30} and N_{30} values in the study area.

2. Seismic Activity and Geological Setting of Kahramanmaras Area

Kahramanmaras basin developed by tectonic-origin surface deformations in the Quaternary and Holocene is located in south of the Bitlis-Poturge Massif area nearby the triple junction of the Arabian, African, and Anatolian plates [9, 10]. Due to the collision of Arabian and Eurasian plates over the Bitlis Suture, the basin was eventually filled out by heavy alluvial sediments and dense turbiditic flysch sequences [11–14]. In the basin, Alacik formation overlies the older units with unconformable contact starting with base conglomerate [15]. In the north, the formation shows different lithological properties that contain marl, clayey limestone, coal band alternations, and claystone. The quaternary age alluviums, dominant materials available in the basin, are composed of gray/light gray, gravel, sand, and silt, which are loose textured and cementless deposited in horizontal and vertical directions. The alluviums thickness in the region was found to increase up to 300 m, which can increase the earthquake intensity by 2-3 degrees [7] (Figure 1).

The collision along Arabian and Anatolian Plates formed the Kahramanmaras territory. The available structural schemes set the triple junction of Arabian, Anatolian, and African plates at the northern Karasu valley, nearby the study area [17]. The study area is surrounded by active faults of the EAFZ (i.e., Surgu Segment, Savrun Segment, Cardak Segment, Toprakkale Segment, Cokak Segment, Amanos Segment, and Golbasi Segment), Kahramanmaras Fault Zone, Engizek Fault Zone, and Narli segment of the Dead Sea Fault Zone (DSFZ) [18]. The Engizek Fault Zone with a length of 66 km locates in north of the study area [19, 20]. The Kahramanmaras Fault Zone (KFZ) begins from east of the study area and passes through the northern part of Kahramanmaras city and extends until the Kilavuzlu Dam [19, 20]. Yilmaz et al. [16] revealed that the Golbasi-Turkoglu segment has suffered from numerous devastating earthquakes (Table 1). An earthquake with a magnitude of 6.8 occurred in 1544 on Cardak Fault [21]. Nalbant et al. [22] studied the KM zone (the area between Kahramanmaras and Malatya), which has gathered significant amount of stress during the last 200 years; thus the magnitude of a possible earthquake along the segment ruptured by 1114 (Mw > 7.8) and 1513 (Mw > 7.4) earthquakes is expected to be larger than 7.3. Palutoglu and Sasmaz [18] pointed out that another destructive earthquake in the vicinity of study area took place in 1795 with a magnitude of 7.0 (Figure 2). Accordingly, Golbasi-Turkoglu Segment, the KFZ, the Engizek Fault, and the Cardak Fault come to the forefront. Therefore, Kahramanmaras and its vicinity area are defined as an area with a seismic gap, and large earthquakes are expected to occur in a near future.

3. Methodology

One of the most widely used surface wave analysis methods to calculate V_{S30} and site response analysis is the Multichannel Analysis of Surface Wave (MASW) method [23, 24]. The MASW is a seismic survey employed to record Rayleigh waves on a multichannel record [25]. Subsurface wave velocities at 88 sites were measured using MASW in the study area by the municipality of Kahramanmaras in order to complete the geophysical studies. The test equipment consists of a 12-channel geometrics seismograph with 4.5 Hz frequency vertical geophones spaced 3 m apart from each other and a sledge hammer with 9 kg weight. Locations, where the 88 MASW tests were carried out, are shown in Figure 3.

Microtremor Array Measurements (MAM) carried out by Ozmen et al. [8] at 10 different locations in the study area were used to estimate the shallow S-wave velocity profiles. The Spatial Auto Correlation (SPAC) method was performed to recover Rayleigh wave phase velocity in a 1–30 Hz frequency range. Microtremor data were recorded simultaneously by means of a 24-bit A/D portable recorder on sensors mounted in the field over various durations. The MAM tests were carried out on the clastic and carbonate rocks except sites 4624 and 4625 lying in a quaternary soil. Ozmen et al. [8] revealed that most of the profiles in the study area have top layers with less than 10 m thickness. V_S of the top layers were found to be high at many sites, apart from three sites (4617, 4624, and 4626) with less than 200 m/s in the study area. Figure 4 shows an inverted 1D S-wave velocity profile up to 100 m depth by means of a hybrid heuristic.

4. Seismic Site Classification for the Kahramanmaras Area

Site classification using NEHRP system is determined based on the average properties of the soil within upper 30 m in the ground, including V_{S30}, N_{30}, and undrained shear strength (s_{u30}) [26]. Table 2 lists the five different site classes in terms of V_{S30} and N_{30} proposed by the NEHRP system. The present investigation proposes a series of SSC maps prepared using a GIS software in order to classify the study area based on V_{S30} for 76 locations and N_{30} for 287 boreholes.

4.1. V_{S30}-Based Seismic Site Classification. V_{S30}, a parameter used for site classification in building codes, can be estimated by dividing 30 m with the required time of the wave travelling over an upper 30 m depth [2, 27]. The V_{S30} values required for the SSC could be estimated by using the following equation [26]:

$$V_{S30} = \frac{30}{\sum_{i=1}^{n} (d_i / V_{si})}, \quad (1)$$

where d_i is the thickness of the i^{th} layer, V_{Si} is V_S of the i^{th} layer, and n is the number of the strata within the upper 30 m.

Boore [28] proposed four different methods to estimate the values of V_{S30} for the profiles which do not have a 30 m depth. The method employed in the present study was the correlation between shallow velocities and V_{S30}, where the key parameter is time-averaged velocity to a certain depth d (V_{Sd}). V_{Sd} can be calculated using the following equation:

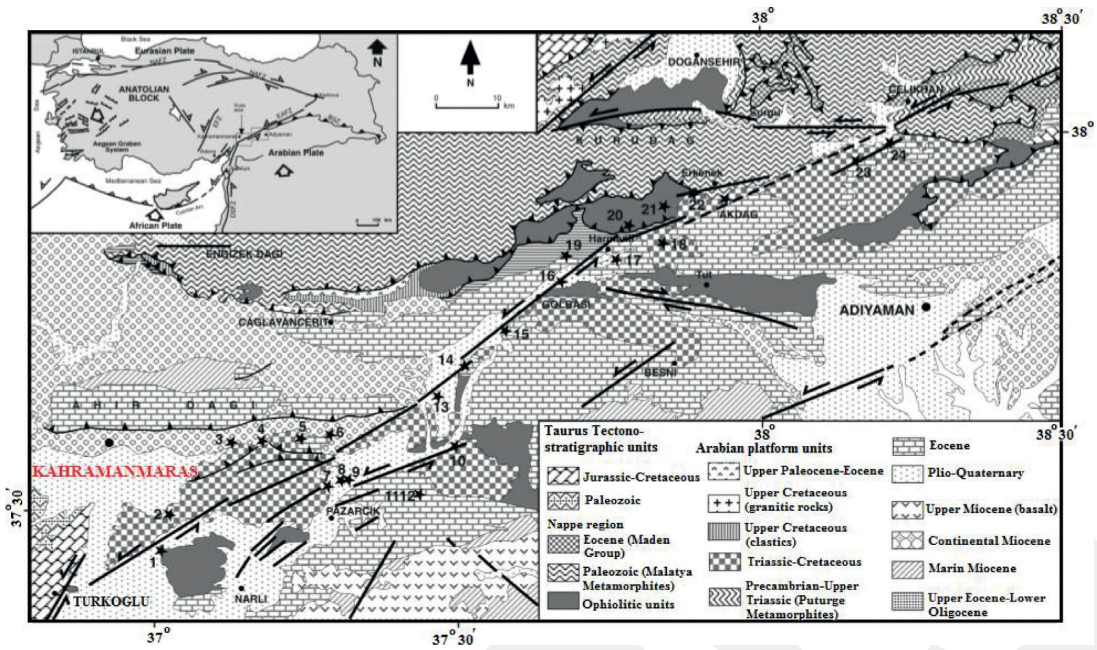

Figure 1: Geological map of the Kahramanmaras area [16].

Table 1: Earthquake events took place on Golbası-Turkoglu segment [16, 22, 38, 39].

Date	Magnitude	Length of rupture (km)
29 November, 1114	$M = 7.8$	—
28 March, 1513	$M = 7.4$	103
2 March, 1893	$M = 7.1$	45
4 December, 1905	$M = 6.8$	38

$$V_s(d) = \frac{d}{tt(d)}, \tag{2}$$

where $tt(d)$ is travel time to a depth d and it is described as follows:

$$tt(d) = \int_0^d \frac{dz}{V_s(z)}. \tag{3}$$

The datasets of 15 MASW and 10 MAM V_S sites with actual depths of measured shear wave velocity models reaching to 30 m were employed to extend the depths with less than 30 m. Actually, V_{S30} for shallow models were estimated by correlating V_{S30} using these readily available 25 sites against their V_{Sd} for the depths (d) assumed. The depths (d) were found to be ranging from 10 m to 24 m in such approach over the study area. As recommended by Boore [28], the authors have ignored the sites with less than a 10 m depth and produced straight regression lines for various depths from 10 m to 24 m (Figure 5). It seems that the results obtained are consistent with those obtained by Boore [28]. As can be seen from Figure 5, coefficient of correlations (R^2) is higher for the larger depths likely because of the increase in effective stress resulting in decrease in void ratio [29–32]. The form of the equations for these regression lines was found to be as follows:

$$\log V_S(30) = a + b \log V_S(d), \tag{4}$$

where V_{S30} is the average shear wave velocity, V_{Sd} is the time-averaged velocity at a certain depth, a and b are the coefficients. The authors have estimated the V_{S30} values for the 76 sites by employing equations (1)–(4) and plotted their findings using ArcGIS software on Figure 6. The V_s estimates made by the authors were found to be consistent with the studies by Biricik and Korkmaz [7], Ozmen et al. [8], and Perincek and Kozlu [12] carried out on the nearby area. It can be seen that the study area was primarily classified as C with a 78% of the entire area, while classes B and D were seen in much narrow regions through the study area.

Figure 7 has been plotted in order to characterize the variation of soil types at the depths of 5 m, 10 m, 15 m, 20 m, and 25 m. A 2.9% of the soils at 5 m depth was classified as E (red regions close to the airport), an 11.6% of those was classified as B, a 39% of those was classified as D, and 46.5% was classified as B (the northern regions) (Figure 7(a)). Similarly, variation of the soil types at a depth of 25 m was found to be about 6.1%, 28.6%, and 65.3% for classes B, D, and C, respectively (Figure 7(e)).

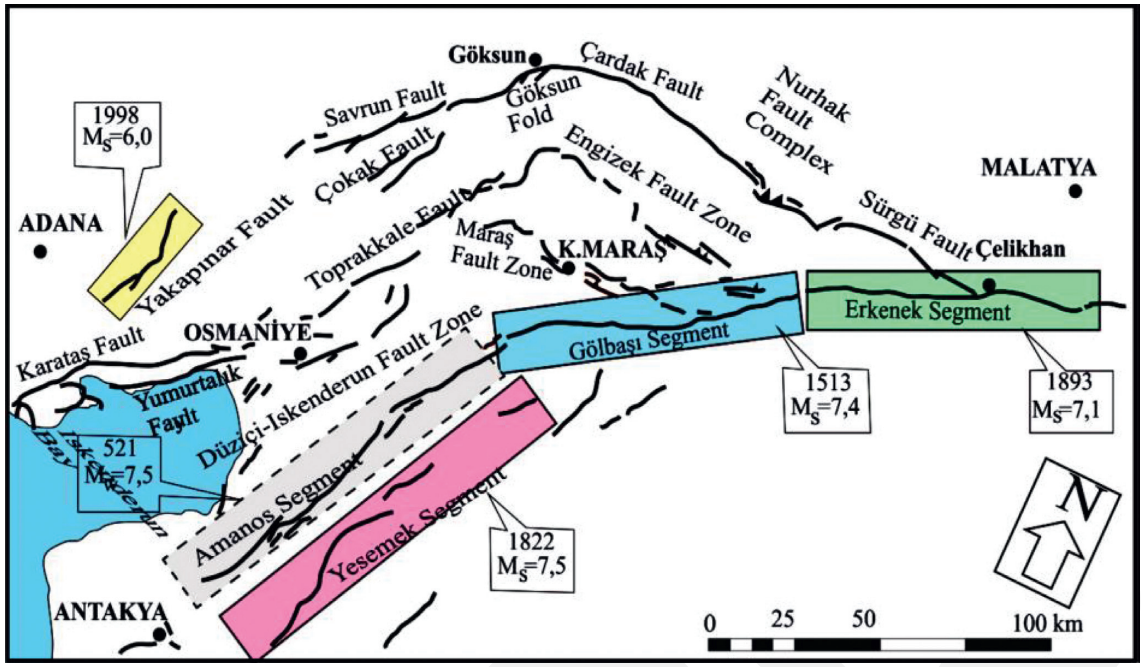

Figure 2: Surface ruptures along the EAFZ [18].

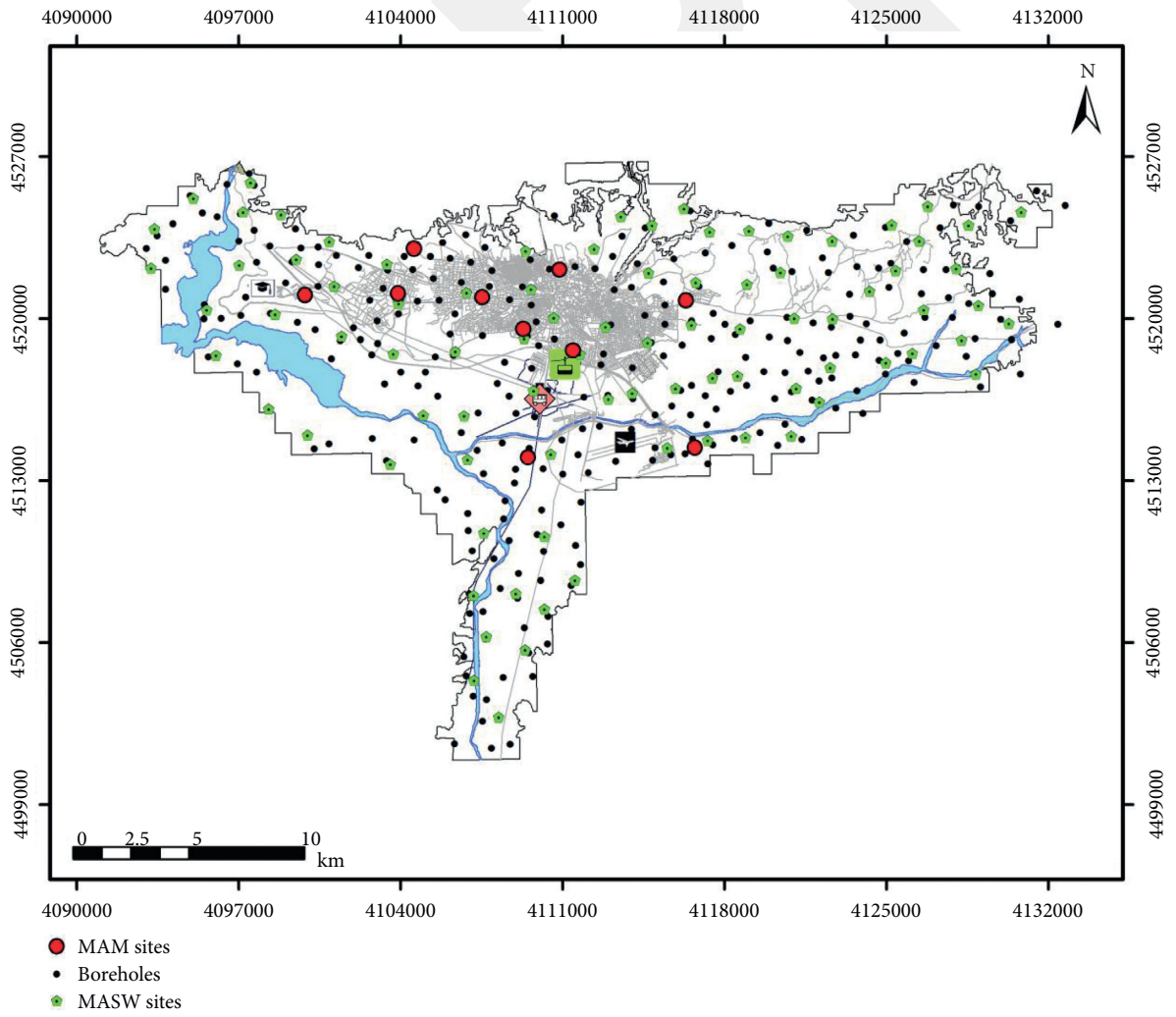

Figure 3: Locations of field tests [8, 10].

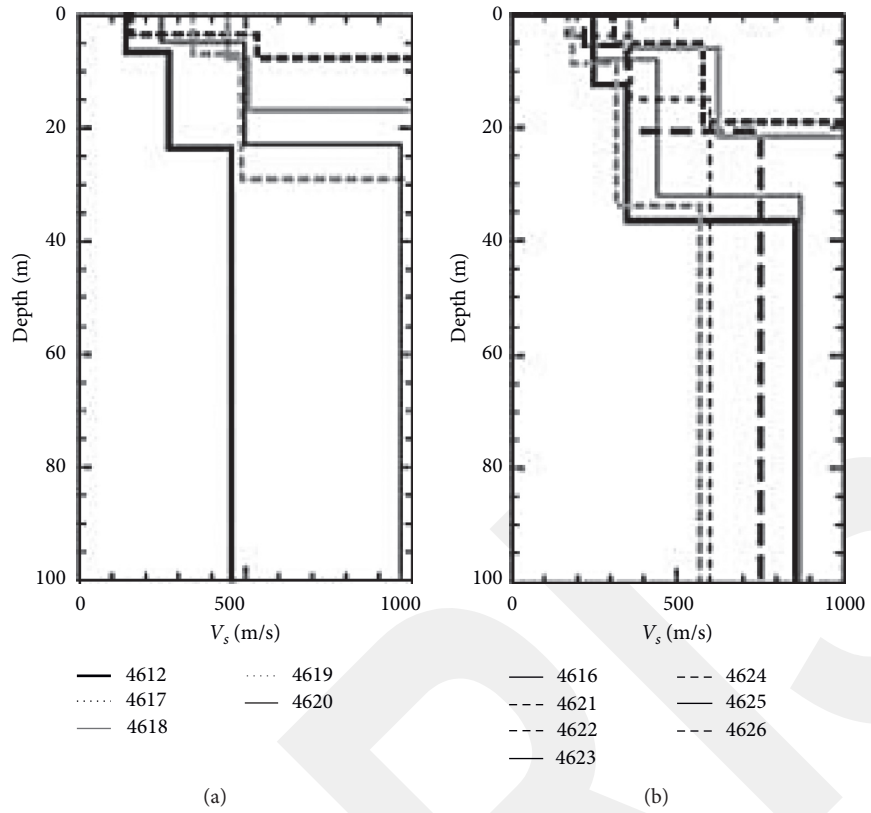

Figure 4: The V_S profiles implemented by MAM test in the study area [8].

Table 2: Definition of NEHRP site classes in terms of V_{S30} and N_{30} [3].

Site class	General description	V_{S30} (m/s)	N_{30}
A	Hard rock	>1500	—
B	Rock	$760 < V_{S30} \leq 1500$	—
C	Very dense soil and soft rock	$360 < V_{S30} \leq 760$	>50
D	Stiff soil	$180 < V_{S30} \leq 360$	$15 \leq N_{30} \leq 50$
E	Soft soil	$V_{S30} < 180$	‘15

4.2. N_{30}-Based Seismic Site Classification. The SPT-N values, which were corrected for hammer energy variation, show the presence of dense to very dense sands across the entire study area apart from Yavuz Selim region, a recently settled industrial area in the southern region, where loose sands with clay and silt inclusions were found. The SPT-N values up to 30 m depth can be estimated by using the equation proposed by Kumar et al. [33] as follows:

$$N_{30} = \frac{\sum_{i=1}^{n} d_i}{\sum_{i=1}^{n} (d_i / N_i)}, \quad (5)$$

where N_{30} is the average SPT-N through 30 m, d_i is thickness of the i^{th} layer, n is number of the layers in 30 m depth, and N_i is the value of SPT-N for layer i. The authors had employed equation (5) in order to generate the SPT-N based SSC maps through the 287 boreholes across the study area. Following N_{30} estimations, the SSC maps over the study area using the NEHRP classification system have been produced (Figure 8) [3]. As can be seen from the Figure 8, 57.5% of the soils were classified as D, while the rest (42.5%) were classified as C. Average SPT-N maps for the depths of 5 m, 10 m, 15 m, 20 m, and 25 m have been plotted in Figure 9. For example, types of the soils at 5 m depth were found to be class E (dark brown colour in the central, southern, and eastern parts), class C (northern parts), and class D with the percentages of 8.4, 11.1, and 80.5, respectively (Figure 9(a)). In general, class D was found to be the dominant soil type at any depth in the study

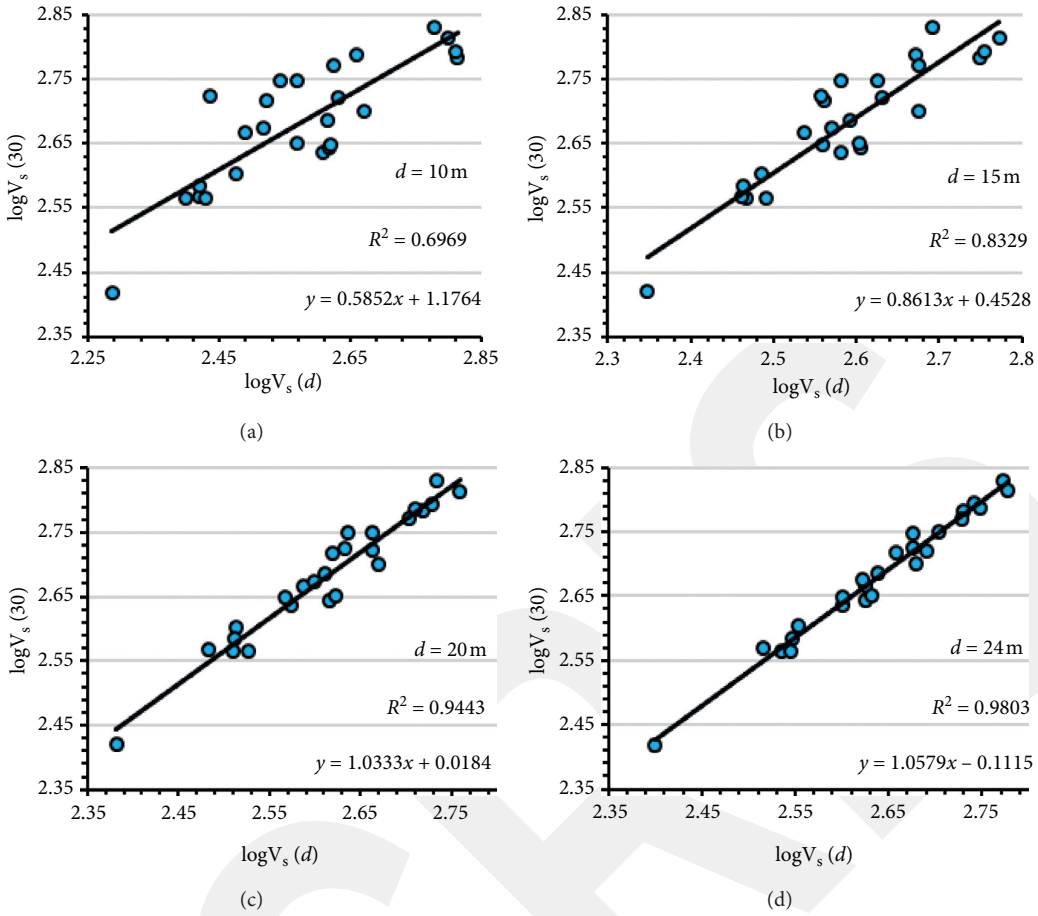

Figure 5: log (V_{S30}) as a function of log (V_{Sd}), for d = 10 m, 15 m, 20 m, and 24 m.

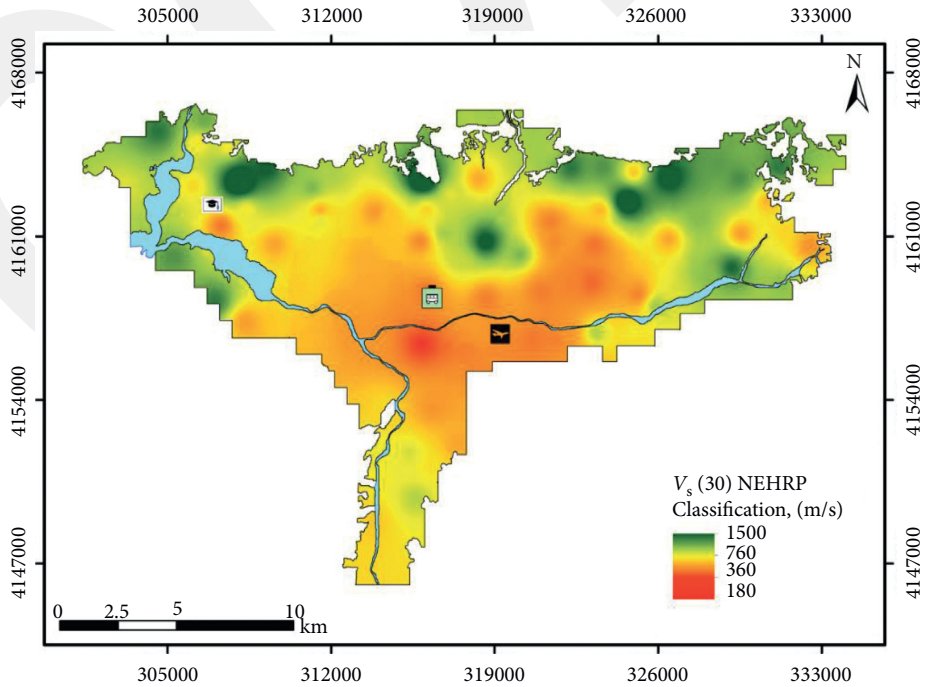

Figure 6: V_{S30} map of Kahramanmaras area.

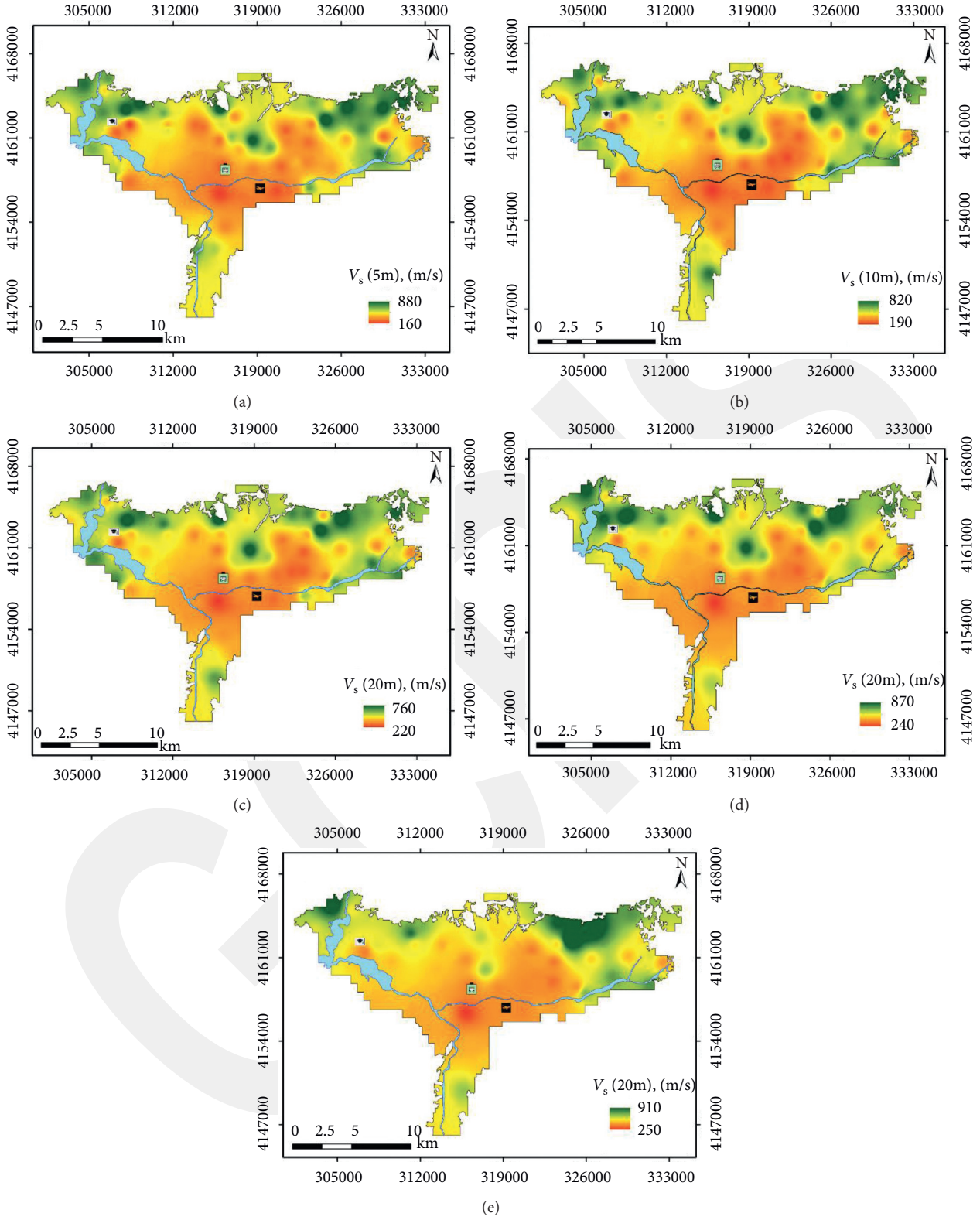

Figure 7: Average V_S values for the depths of (a) 5 m, (b) 10 m, (c) 15 m, (d) 20 m, and (e) 25 m in Kahramanmaras area.

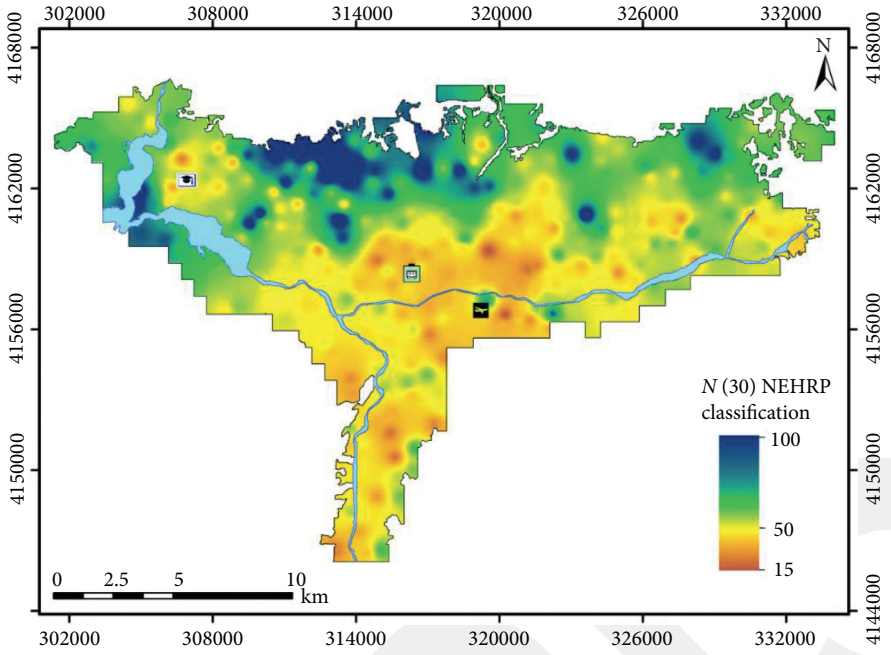

Figure 8: N_{30} based seismic site classification map in Kahramanmaras area.

area. Soft soil deposits were mainly observed at relatively shallow depths in the study, and their amounts were decreased by increasing depth.

5. Spatial Variability of Rock Depth

Classification of rock based on the shear wave velocity (V_S) in geotechnical earthquake engineering is still in practice. According to the NEHRP classification system, soft rock and very dense soil at upper 30 m have the average velocities of 360 m/s to 760 m/s. The 30 m average V_S of a value more than 760 m/s is classified as a hard rock [34]. For the purpose of seismic microzonation, Nath [35] defined the seismic bed rock with an average V_S value of 3000 m/s and higher and from 400 m/s to 700 m/s for the engineering bed rock. Miller et al. [36] had assigned the level of bed rock through considering V_S as 244 m/s and above by using MASW survey. For the present study, velocity of shear wave of 330 ± 30 m/s has been specified for the weathered rock (WR) and 760 ± 60 m/s has been appointed for the engineering rock (ER). Among the 98 V_S locations for the MASW and MAM surveys, only 83 locations were able to be utilized to assign the upper level of the stratum corresponding to V_S of 330 ± 30 m/s. The estimated depths were tabulated (Table 3) and employed to generate the map for weathered rock level up to 14 m depth via ArcGIS Software V 10.4.1 (Figure 10). About 67% of the region has weathered rock level at the entire ground surface except the central part and a small area at the eastern side. The weathered rock level between 0 m and 5 m was estimated about 17.7% of the region. About 12.7% of the region was observed with weathered rock from 5 m to 10 m depth (dark orange colour). Around 2.6% of the region has weathered rock level from 10 m to 14 m (around the airport). In general, more than half of the study area was found to be a very dense soil or soft rock at the surface. Engineering bed rock strata were observed at 52 different locations, where V_S values correspond to 760 ± 60 m/s. Data in those locations have been employed to generate the map of engineering bed rock level (Figure 11). Engineering bed rock level in the study area was found to be at the ground level in northern region (Ahir Dagi mountain) with a percentage of 9.7% of the boreholes. Depth of the engineering rock between 0 m and 10 m depth in the northern-central and western regions was about 17.3% of the whole boreholes. Almost half of the study area (48%) has an engineering depth ranging from 10 m to 20 m (dark green color). The engineering rock level was found to be between 20 m and 32 m for 23% of the entire study area (light green colour). For a depth greater than 100 m, the engineering rock level was found to be about 1.92% of the whole data (site 4624 shown in brown colour).

Figures 12 and 13 present the overburden soil depth to the weathered rock and engineering bed rock levels, respectively. The equivalent V_S for the depth of soil is indicated as V_H and computed as follows [37]:

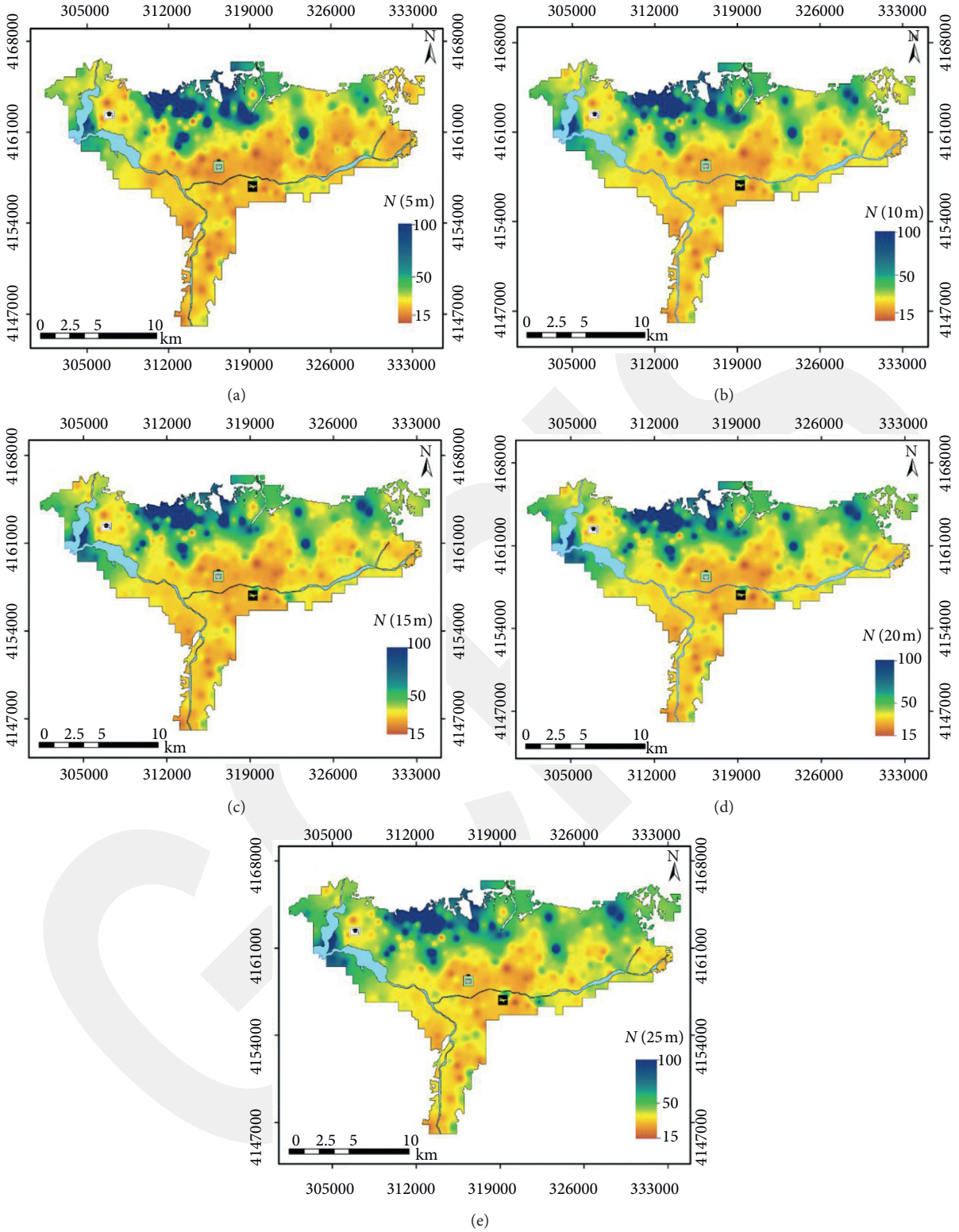

Figure 9: Average SPT-N values for the depths of (a) 5 m, (b) 10 m, (c) 15 m, (d) 20 m, and (e) 25 m in Kahramanmaras area.

Table 3: Coordinates of MASW and MAM test stations implemented in Kahramanmaras city with depth and equivalent shear wave velocity corresponding to weathered and engineering rock.

Station no.	Coordinates		Depth of V_S profile (m)	Depth of rock (m)		Equivalent V_S of the overburden (m/s)	
	X	Y		Weathered	Engineering	Weathered	Engineering
JF-1	303102	4163134	30	0	17.7	*	426
JF-2	303243	4164482	6.7	0	5.4	*	461
JF-3	304612	4165479	21	0	16.4	*	589
JF-4	306579	4165972	22	0	No hard rock	*	*
JF-5	306304	4164973	30	0	18.4	*	399
JF-6	307600	4164862	30	0	21.2	*	469
JF-7	306123	4163156	10	0	No hard rock	*	*
JF-8	304969	4161664	8	0	No hard rock	*	*
JF-9	307315	4161457	20	5.1	No hard rock	230	*
JF-10	309583	4160651	30	0	No hard rock	*	*
JF-11	309361	4162365	5.5	0	No hard rock	*	*
JF-12	308079	4163319	22	No soft rock	0	*	*
JF-13	309225	4163890	19	No soft rock	0	*	*
JF-14	305264	4160104	16	0	12.7	*	542
JF-15	307030	4158237	19	0	8.8	*	688
JF-16	308332	4157312	24	5.9	No hard rock	155	*
JF-17	311198	4163072	13	0	10.23	*	537
JF-18	311562	4161736	10	0	No hard rock	*	*
JF-19	313897	4162043	18	4.38	No hard rock	231	*
JF-20	316116	4162115	22	0	17	*	374
JF-21	—	—	—	—	—	—	—
JF-22	315959	4163436	22	No soft rock	0	*	*
JF-23	318307	4163431	30	0	No hard rock	*	*
JF-24	319257	4164531	7.5	0	No hard rock	*	*
JF-25	318626	4160774	21	No soft rock	0	*	*
JF-26	316877	4161116	9.5	0	7.4	*	516
JF-27	313473	4160054	30	0	21.3	*	373
JF-28	311344	4160024	10	0	No hard rock	*	*
JF-29	318676	4158305	30	9.2	No hard rock	242	*
JF-30	316671	4156466	5.5	No soft rock	No hard rock	No hard rock	*
JF-31	316124	4158640	13	9.9	No hard rock	233	*
JF-32	313724	4157835	6	4.82	No hard rock	270	*
JF-33	313797	4156346	10	7.89	No hard rock	256	*
JF-34	311148	4156250	7	No soft rock	No hard rock	No hard rock	*
JF-35	312319	4157883	8	0	6.4	*	391
JF-36	314315	4153826	12	0	9.7	*	364
JF-37	316375	4153663	11.5	0	No hard rock	*	*
JF-38	316335	4151192	10.5	0	No hard rock	*	*
JF-39	315632	4149807	30	0	23	*	523
JF-40	314682	4147511	6.5	0	No hard rock	*	*
JF-41	315362	4151723	19	0	15	*	428
JF-42	314314	4150279	8.5	0	No hard rock	*	*
JF-43	317396	4152137	14	0	No hard rock	*	*
JF-44	320319	4164198	9	0	6.9	*	450
JF-45	321427	4164746	20	0	11.8	*	414
JF-46	320160	4162571	6.5	0	5	*	301
JF-47	322281	4163946	19	0	8.72	*	510
JF-48	323630	4163955	16	0	12.7	*	544
JF-49	303102	4163134	20	0	15.4	*	356
JF-50	303243	4164482	19	No soft rock	0	*	*
JF-51	304612	4165479	15	11.7	No hard rock	232	*
JF-52	306579	4165972	11	8.7	No hard rock	260	*
JF-53	306304	4164973	6.5	No soft rock	No hard rock	No hard rock	*
JF-54	307600	4164862	30	8.5	19.4	304	381
JF-55	306123	4163156	8	0	No hard rock	No hard rock	*
JF-56	304969	4161664	19	0	15.2	*	505
JF-57	307315	4161457	6.5	3.9	No hard rock	187	*

Table 3: Continued.

Station no.	Coordinates		Depth of V_S profile (m)	Depth of rock (m)		Equivalent V_S of the overburden (m/s)	
	X	Y		Weathered	Engineering	Weathered	Engineering
JF-58	309583	4160651	10	No soft rock	No hard rock	No hard rock	*
JF-59	309361	4162365	22	10	13.2	209	239
JF-60	308079	4163319	18	14	No hard rock	257	*
JF-61	309225	4163890	22	13.62	No hard rock	305	*
JF-62	305264	4160104	15	0	11.6	*	438
JF-63	307030	4158237	11	0	No hard rock	*	*
JF-64	308332	4157312	16	9.46	No hard rock	261	*
JF-65	311198	4163072	10	No soft rock	No hard rock	*	*
JF-66	311562	4161736	17	No soft rock	0	*	*
JF-67	313897	4162043	18	0	10.6	*	492
JF-68	316116	4162115	12	No soft rock	0	*	*
JF-69	329780	4164666	30	0	16.8	*	504
JF-70	315959	4163436	22	No soft rock	0	*	*
JF-71	318307	4163431	7	0	No hard rock	*	*
JF-72	319257	4164531	7	0	No hard rock	*	*
JF-73	318626	4160774	10	0	7.8	*	624
JF-74	316877	4161116	13	0	No hard rock	*	*
JF-75	313473	4160054	9	0	No hard rock	*	*
JF-76	311344	4160024	30	0	22.8	*	535
JF-77	318676	4158305	23	0	18.2	*	512
JF-78	316671	4156466	18	No soft rock	0	*	*
JF-79	316124	4158640	6	4.65	No hard rock	261	*
JF-80	313724	4157835	30	0	21.4	*	572
JF-81	313797	4156346	30	8.9	20.5	298	328
JF-82	311148	4156250	15	0	No hard rock	*	*
JF-83	312319	4157883	30	0	No hard rock	*	*
JF-84	314315	4153826	22	5.5	17	236	325
JF-85	316375	4153663	7.5	5.8	No hard rock	273	*
JF-86	316335	4151192	8.7	4.1	No hard rock	270	*
JF-87	315632	4149807	14	0	11.4	*	417
JF-88	314682	4147511	30	0	22.8	*	423
JF-4617	308369	4162107	100	3.8	7.6	140	222
JF-4618	312120	4163601	100	0	17	443	473
JF-4619	311549	4162084	100	0	28.8	*	437
JF-4620	314432	4161874	100	5	22.8	245	407
JF-4621	317106	4162758	100	0	18.5	*	441
JF-4622	321422	4161623	100	6	21	210	299
JF-4623	317503	4159998	100	0	23	*	508
JF-4624	315881	4156383	100	8.5	No hard rock	170	*
JF-4625	321617	4156597	100	8	32	220	364
JF-4626	315822	4160779	100	4	No hard rock	230	*

$$V_H = \frac{\sum_{i=1}^{n} d_i}{\sum_{i=1}^{di} [d_i / V_{si}]}, \quad (6)$$

where $H = \sum$ and d_i is accumulative depth up to the level of weathered rock or engineering bed rock levels in m; d_i and v_{si} indicate the thickness in meters and velocity of shear wave of the i^{th} layer in m/s, respectively. Applying equation (6) has revealed equivalent velocity of the overburden soil ranging from 140 m/s to 443 m/s up to weathered rock and from 222 m/s to 688 m/s up to engineering bed rock. According to the NEHRP classification system, about 85% of the study area has an average overburden V_S from 180 m/s to 360 m/s and is classified as stiff soil over a depth ranging from 3.9 m to 14 m. 11% of the study area has an average V_S less than 180 m/s and is classified as soft soil over a depth from 3.8 m to 8.5 m (yellow areas in Figure 12). Also, average V_S value from ground surface to weathered rock level over the 3.8% of the study area was estimated as higher than 360 m/s.

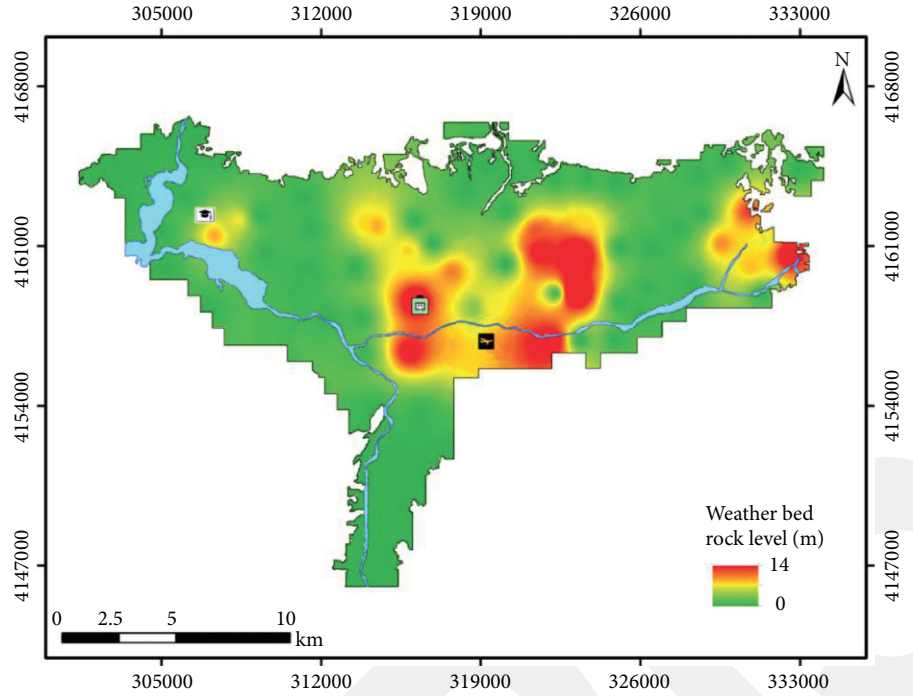

Figure 10: Weathered rock level in Kahramanmaras area using the MASW and MAM data.

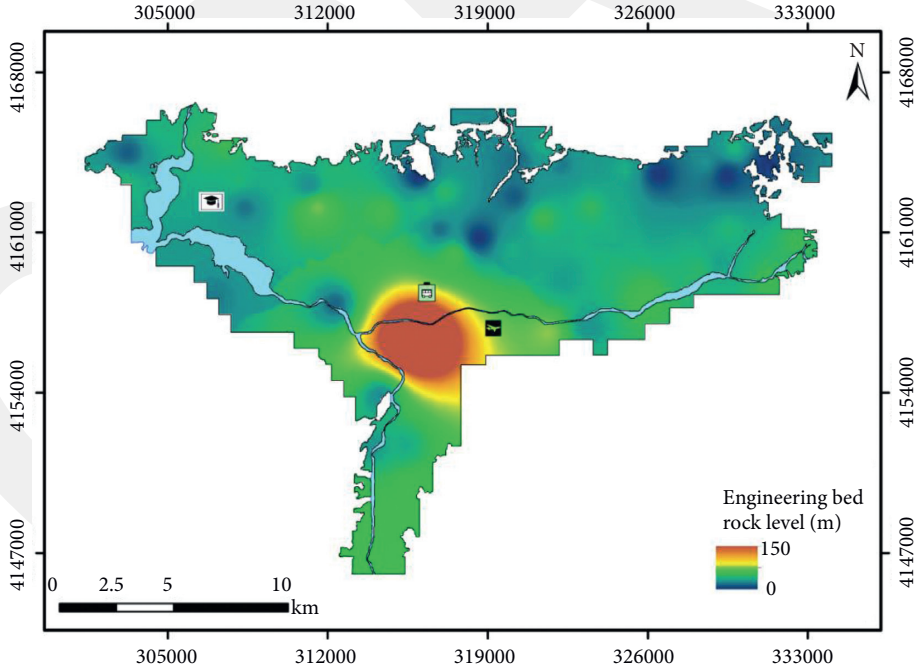

Figure 11: Engineering rock level in Kahramanmaras area using the MASW and MAM data.

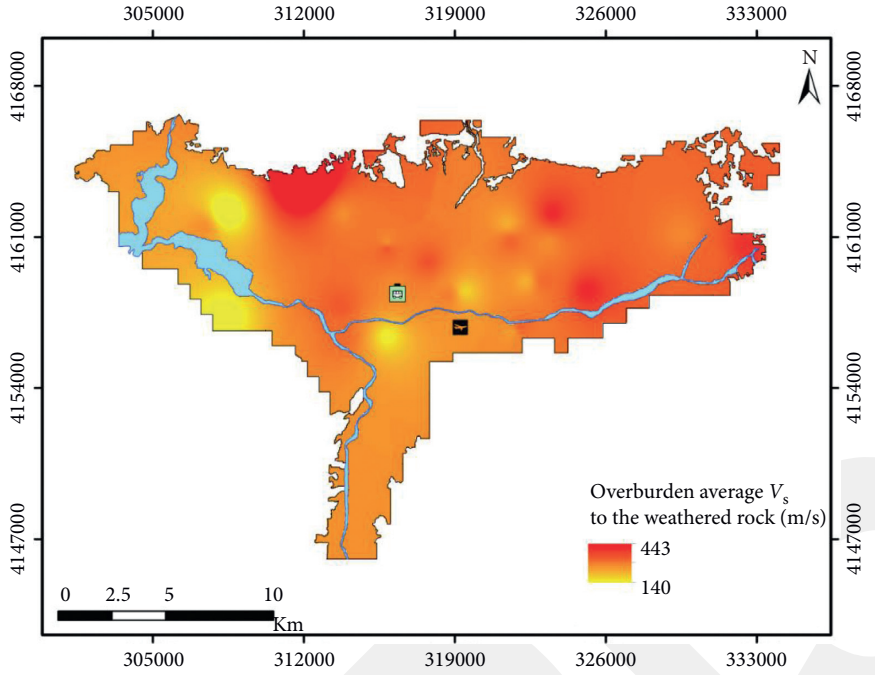

Figure 12: Average V_S of overburden soil to the weathered bed rock in Kahramanmaras area.

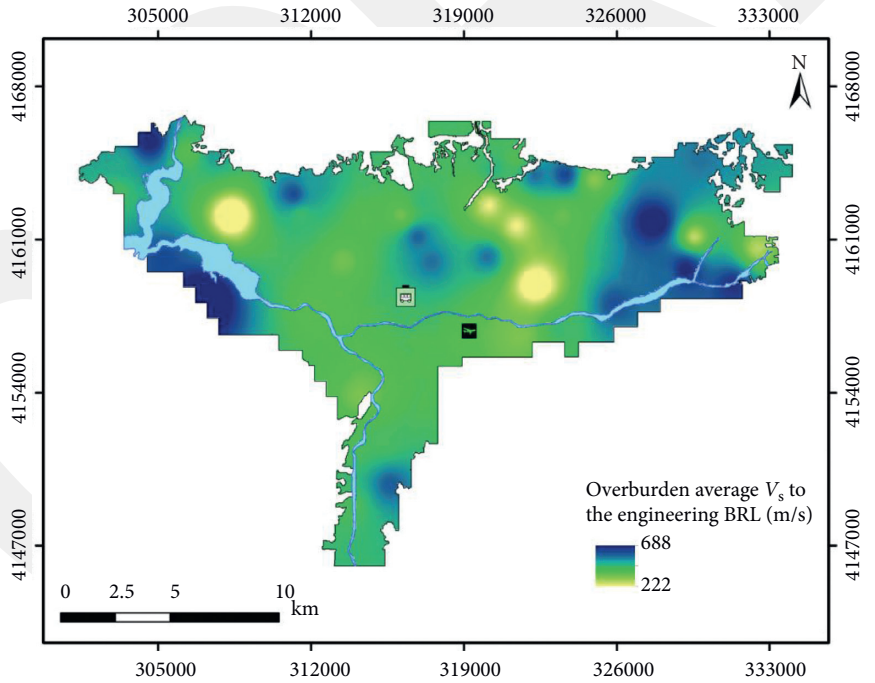

Figure 13: Average V_S of overburden soil to the engineering bed rock of Kahramanmaras area.

Furthermore, average V_S value for the dense overburden soil and/or soft rock from 5 m to 32 m depth, about 85% of the study area, was found to be more than 360 m/s.

6. Conclusions

The purpose of this study is to generate an intensive series of Geographic Information System (GIS) maps for the seismic site classification (SSC) in Kahramanmaras city, influenced by both west part of East Anatolian Fault and northern part of Dead Sea Fault Zones with a capability of producing the strongest future earthquakes in southern-central Turkey. The study presents the GIS maps for average SPT-N values (N_{30}), average shear wave velocity values (V_{S30}), variation in depths to weathered and engineering rock levels, and average V_S of overburden soil. The V_{S30} based SSC maps indicated that majority of the soils in the study area were found to be class C, although N_{30} based SSC maps indicated that more than 50% of the study area was class D. The differences among the findings by two different approaches could be explained by the accuracy of both geophysical tests of MASW and MAM at the field because of some difficulties in opening 287 boreholes and recording their SPT-N drops. Another reason could be the method employed for extending the V_S profiles up to 30 m. This approach increases the queries on consistency of NEHRP classification system. Furthermore, another series of raster maps generated for average V_S and SPT-N values at 5 m, 10 m, 15 m, 20 m, and 25 m depths revealed that 85% of the study area, according to the weathered bed rock level, was classified as soil type D with depths ranging from 3.9 m to 14 m, while 84% of the study area, according to the engineering bed rock level, was classified as C from 5 m to 32 m depth.

Data Availability

The Global Centroid Moment Tensor Project database was searched using http://www.globalcmt.org/CMTsearch.html (last accessed May 2019).

Conflicts of Interest

The authors declare that they have no conflicts of interest.

References

[1] K. Pitilakis, *Site Effects in Recent Advances in EarthquakeGeotechnical Engineering and Microzonation*, A. Ansal, Ed., vol. 368, pp. 139–197, Kluwer Academic Publications, Dordrecht, Netherlands, 2004.

[2] Building Seismic Safety Council (BSSC), *NEHRP Recommended Provisions for Seismic Regulations for New Buildings and Other Structures, 2000 Edition, Part 1: Provisions," Prepared by the Building SeismicSafety Council for the Federal Emergency Management Agency (Report FEMA 368)*, Building Seismic Safety Council (BSSC), Washington, D.C., USA, 2001.

[3] Building Seismic Safety Council (BSSC), *NEHRP Recommended Provision for Seismic Regulation for New Buildings and Other Structures (FEMA 450), Part 1: Provisions," Building Safety Seismic Council for the Federal Emergency Management Agency*, Building Seismic Safety Council (BSSC), Washington, DC, USA, 2003.

[4] International Codes Council, *International Building Code (IBC)*, International Codes Council, Washington, DC, USA, 2009.

[5] D. M. Boore, W. B. Joyner, and T. E. Fumal, "Equations for estimating horizontal response spectra and peak acceleration from western North American earthquakes: a summary of recent work," *Seismological Research Letters*, vol. 68, no. 1, pp. 128–153, 1997.

[6] C. J. WillsM. W. Petersen et al., "A site-conditions map for California based on geology and shear-wave velocity," *Bulletin of the Seismological Society of America*, vol. 90, pp. S187–S208, 2000.

[7] A. S. Biricik and H. Korkmaz, "The seismicity of kahramanmaraş, eastern mediterannean- Turkey," *Marmara Coğrafya Dergisi*, vol. 1, pp. 53–82, 2001.

[8] T. O. Ozmen, H. Yamanaka, M. A. Alkan, U. Ceken, T. Ozturk, and H. Sezen, "Microtremor Array measurements for shallow S-wave profiles at strong-motion stations in hatay and Kahramanmaras provinces, southern Turkey," *Bulletin of the Seismological Society of America*, vol. 107, pp. 1–11, 2017.

[9] S. K. Husing, W. J. Zachariasse, D. J. J. Hinsbergen et al., *Oligocene–Miocene basin evolution in SE Anatolia, Turkey: constraints on the closure of the eastern Tethys gateway*, vol. 311, pp. 107–132, Geological Society, London, UK, 2009.

[10] B. Akil and B. Y. Ecemis, *Geological-Geotechnical Study Report for the Municipality of Kahramanmaras*, Directorate of Underground Studies Department, Mineral Research & Exploration General Directorate, (MTA), Ankara, Turkey, 2011.

[11] A. M. C. Sengor and Y. Yilmaz, "Tethyan evolution of Turkey; A plate tectonic approach," *Tectonophysics*, vol. 75, pp. 181–241, 1981.

[12] D. Perincek and H. Kozlu, "Stratigraphy and structural relations of the units in the Afşin-Elbistan-Doğanşehir region (Eastern Taurus)," in *Proceedings of the International Symposium, Geology of Taurus Belt*, O. Tekeli and M. C. Goncuoglu, Eds., pp. 181–198, MTA, Ankara, Turkey, 1984.

[13] D. E. Karig and H. Kozlu, "Late Palaeogene-Neogene evolution of the triple junction region near Maraş, south-central Turkey," *Journal of the Geological Society*, vol. 147, no. 6, pp. 1023–1034, 1990.

[14] Y. Yilmaz, "New evidence and model on the evolution of the southeast Anatolian orogen," *Geological Society of America Bulletin*, vol. 105, no. 2, pp. 251–271, 1993.

[15] M. Gul, G. Darbas, and K. Gurbus, "Tectono-stratigraphic position of Alacik formation (latest middle eocene-early miocene) in the kahraman maras basin," in *Turkish with English Abstract and Summary*, vol. 18, pp. 183–197, Istanbul University Mühendislik Fakültesi Yerbilimleri Dergisi, Istanbul, Turkey, 2005.

[16] H. Yilmaz, S. Over, and S. Ozden, "Kinematics of the east Anatolian Fault zone between turkoglu (Kahramanmaras) and celikhan (adiyaman), eastern Turkey," *Earth, Planets and Space*, vol. 58, no. 11, pp. 1463–1473, 2006.

[17] A. M. C. Sengor, N. Gorur, and F. Saroglu, "Strike-slip faulting and related basin formation in zones of tectonic escape: Turkey as a case study," *Special publication-Society of Economic Paleontologists and Mineralogists*, vol. 37, pp. 227–264, 1985.

[18] M. Palutoglu and A. Sasmaz, "29 november 1795 kahramanmaraş earthquake, southern Turkey," *Bulletin of The Mineral Research and Exploration*, vol. 155, pp. 191–206, 2017.

[19] O. Emre, T. Y. Duman, and H. Elmaci, *1:250.000 Olcekli Turkiye Diri Fay Haritasi Serisi. Elbistan (NJ 37-5) Sheet Seri No:37*, General Directorate of Mineral and Exploration, Ankara, Turkey, 2012a.

[20] O. Emre, T. Y. Duman, S. Olgun, H. Elmaci, and S. Ozalp, *1: 250.000 Olcekli Türkiye Diri Fay Haritasi Serisi. Gaziantep (NJ 37-9) Sheet Seri No: 38*, General Directorate of Mineral and Exploration, Ankara, Turkey, 2012b.

[21] N. V. Kondorskaya and V. I. Ulomov, "Special Catalogue of Earthquakes of the Northern Eurasia (SECNE)," *Joint Institute of Physics of the Earth (JIPE), Russian Academy of Sciences*, Moscow, Russia, 1999.

[22] S. S. Nalbant, J. McCloskey, S. Steacy, and A. A. Barka, "Stress accumulation and increased seismic risk in eastern Turkey," *Earth and Planetary Science Letters*, vol. 195, no. 3-4, pp. 291–298, 2002.

[23] P. Anbazhagan, A. Kumar, and T. G. Sitharam, "Seismic site classification and correlation between standard penetration test N value and shear wave velocity for lucknow city in indo-gangetic basin," *Pure and Applied Geophysics*, vol. 170, no. 3, pp. 299–318, 2013.

[24] H. B. Ozmen, M. Inel, E. Akyol, B. T. Cayci, and H. Un, "Evaluations on the relation of RC building damages with structural parameters after May 19, 2011 Simav (Turkey) earthquake," *Natural Hazards*, vol. 71, no. 1, pp. 63–84, 2014.

[25] C. B. Park, J. Xia, and R. D. Miller, "Estimation of near-surface shear-wave velocity by inversion of Rayleigh wave," *Geophysics*, vol. 64, no. 3, pp. 691–700, 1999.

[26] R. D. Borcherdt, "Estimates of site-dependent response spectra for design (methodology and justification)," *Earthquake Spectra*, vol. 10, no. 4, pp. 617–653, 1994.

[27] R. Dobry, R. D. Borcherdt, C. B. Crouse et al., "New site coefficients and site classification system used in recent building seismic code provisions," *Earthquake Spectra*, vol. 16, no. 1, pp. 41–67, 2000.

[28] D. M. Boore, "Estimating s (30) (or NEHRP site classes) from shallow velocity models (depths)," *Bulletin of the Seismological Society of America*, vol. 94, no. 2, pp. 591–597, 2004.

[29] B. O. Hardin and F. E. Richart Jr., "Elastic wave velocity in granular soils," *Journal of Soil Mechanics and Foundation Division, ASCE*, vol. 89, no. 1, pp. 33–65, 1963.

[30] J. P. Sully and R. G. Campanella, "Evaluation of in situ anisotropy from crosshole and downhole shear wave velocity measurements," *Géotechnique*, vol. 45, no. 2, pp. 267–238, 1995.

[31] M. C. Matthews, V. S. Hope, and C. R. I. Clayton, "The use of surface waves in the determination of ground stiffness profiles," *Proceedings of the Institution of Civil Engineers-Geotechnical Engineering*, vol. 119, no. 2, pp. 84–95, 1996.

[32] E. Brignoli, M. Gotti, and K. H. Stokoe, "Measurement of shear waves in laboratory specimens by means of piezoelectric transducers," *Geotechnical Testing Journal*, vol. 19, no. 4, pp. 384–397, 1996.

[33] A. Kumar, N. H. Harinarayan, V. Verma, S. Anand, U. Borah, and M. Bania, "Seismic site classification and empirical correlation between standard penetration test N value and shear wave velocity for guwahati based on thorough subsoil investigation data," *Pure and Applied Geophysics*, vol. 175, 2018.

[34] P. Anbazhagan and T. G. Sitharam, "Spatial variability of the depth of weathered and engineering bedrock using multichannel analysis of surface wave method," *Pure and Applied Geophysics*, vol. 166, no. 3, pp. 409–428, 2009.

[35] S. K. Nath, "Seismic microzonation framework-principles and applications," in *Proceedings of the Workshop on Microzonation*, pp. 9–35, Indian Institute of Science, Bangalore, India, May 2007.

[36] R. D. Miller, J. Xia, C. B. Park, and J. M. Ivanov, "Multichannel analysis of surface waves to map bedrock," *The Leading Edge*, vol. 18, no. 12, pp. 1392–1396, 1999.

[37] A. I. Kanli, P. Tildy, Z. Pronay, A. Pinar, and L. Hemann, "V_{S30} mapping and soil classification for seismic site effect evaluation in Dinar region, SW Turkey," *Geophysical Journal International*, vol. 165, pp. 223–235, 2006.

[38] N. N. Ambraseys, "Temporary seismic quiescence: SE Turkey," *Geophysical Journal*, vol. 96, pp. 311–331, 1988.

[39] N. N. Ambraseys and J. A. Jackson, "Faulting associated with historical and recent earthquakes in the eastern Mediterranean region," *Geophysical Journal International*, vol. 133, no. 2, pp. 390–406, 1998.